



Research article

Evaluation of the most optimal multiparametric magnetic resonance imaging sequence for determining pathological length of capsular contact



Aslıhan Onay^{a,*}, Metin Vural^b, Ayşe Armutlu^c, Sevda Özel Yıldız^d, Murat Can Kiremitçie, Tarık Esen^f, Barış Bakır^g

^a Department of Radiology, Baskent University School of Medicine, Marasel Fevzi Cakmak Blvd, No: 45, Ankara, Turkey

^b Department of Radiology, VKF American Hospital, Tesvikiye, Güzelbahçe Street, No:20 Sisli, 34365, Istanbul, Turkey

^c Department of Pathology, Koç University Hospital, Topkapı, Davutpasa Blvd., No. 4 Zeytinburnu, 34010, Istanbul, Turkey

^d Department of Biostatistics, Istanbul University Istanbul Faculty of Medicine, Istanbul Medical Faculty, Capa, Fatih, 34093, Istanbul, Turkey

^e Department of Urology, Koç University Hospital, Topkapı, Davutpasa Blvd. No. 4 Zeytinburnu, 34010, Istanbul, Turkey

^f Department of Urology, Koc University School of Medicine, Topkapı, Davutpasa Blvd. No. 4 Zeytinburnu, 34010, Istanbul, Turkey

^g Department of Radiology, Istanbul University Istanbul School of Medicine, Istanbul Medical Faculty, Capa, Fatih, 34093, Istanbul, Turkey

ARTICLE INFO

Keywords:

Prostate cancer

Multi-parametric prostate MRI

Extracapsular extension

Length of capsular contact

ABSTRACT

Objectives: To assess the most optimal multi-parametric magnetic resonance imaging sequence (Mp-MRI) in determining pathological length of capsular contact (LCC) for the diagnosis of prostate cancer extraprostatic extension (EPE).

Methods: 105 patients with prostate cancer who underwent Mp-MRI of prostate prior to radical prostatectomy were enrolled in this retrospective study. LCC was determined from T2-weighted images (T2WI), Apparent Diffusion Coefficient (ADC) map, dynamic contrast-enhanced MRI (DCE-MRI) separately by two blinded radiologists. The LCCs in patients with and without EPE were compared with Mann Whitney-U test. The relationship between pathological LCC and the LCC that was measured from each Mp-MRI sequences were calculated by using Spearman test. The ability of all individual Mp-MRI sequences in determining pathological LCC was calculated by drawing receiver operator characteristic (ROC) curves. The diagnostic accuracy of LCC based on each MRI sequences for EPE diagnosis was also calculated with ROC curve analysis.

Results: The patients with EPE had longer median LCC than patients without EPE for each Mp-MRI sequences and for both readers. In addition, the LCC showed a broader overlapping between patients with and without EPE on ADC map (reader-1, $p = 0.01$; reader-2, $p = 0.01$) when compared with T2WI (reader-1, $p = 0.002$; reader-2, $p = 0.001$) and DCE-MRI (reader-1, $p = 0.001$; reader-2, $p = 0.001$). LCC based on DCE-MRI showed the strongest correlation with pathological LCC. The area under the curve (AUC) based on LCC was higher when using the DCE-MRI (reader-1: 0.874, $p = 0.030$; reader-2: 0.862, $p = 0.02$) than when using T2WI and ADC map in predicting pathological LCC for both readers. While the LCC based on ADC map showed poor diagnostic accuracy, LCC based on T2WI and DCE-MRI had fair diagnostic accuracy for EPE diagnosis.

Conclusion: The contact between prostate tumor and capsule seems to be a useful and objective parameter for evaluating the EPE of prostate cancer with Mp-MRI. More specifically, LCC based on DCE-MRI has highest correlation with pathological LCC and has better ability to predict pathological LCC when compared with other Mp-MRI sequences. However, the performance of LCC based on T2WI and DCE-MRI was similar for EPE diagnosis. It seems measurement of LCC from DCE-MRI and measurement of LCC from T2WI does not show any difference in clinical EPE assessment.

1. Introduction

Accurate local staging of prostate cancer (PCa) is of clinical importance. PCa with extraprostatic extension (EPE) is associated with a higher risk of positive surgical margin, biochemical recurrence and

worsened overall prognosis after radical prostatectomy (RP) when compared with organ confined disease [1–3]. Knowledge of possible EPE has potential influence on choosing the appropriate surgical approach (neurovascular bundle-sparing procedures or wide resection margins) and even the best treatment modality [4]. Clinical staging of

* Corresponding author at: Department of Radiology, Baskent University School of Medicine, Marasel Fevzi Cakmak, No: 45 Cankaya, Ankara, Turkey.

E-mail address: aslionay@gmail.com (A. Onay).

<https://doi.org/10.1016/j.ejrad.2019.01.020>

Received 13 November 2018; Received in revised form 20 January 2019; Accepted 21 January 2019

0720-048X/© 2019 Elsevier B.V. All rights reserved.

PCa made by digital rectal examination or clinical nanograms, which were additionally based on serum prostate specific antigen (PSA) and preoperative biopsy Gleason score have low specificity and sensitivity with potentially inaccurate assessment about the volume, extent and aggressiveness of prostate tumor [5].

Multiparametric magnetic resonance imaging (Mp-MRI) is the reference standard imaging modality for local staging of PCa [6–8]. However, the revealed accuracy of Mp-MRI for evaluation of EPE ranged widely [9]. The inconsistency of the results might be associated with the subjective nature of EPE assesment that was based on visual evaluation of secondary findings such as abutment, irregularity or bulging of the prostate capsule and thickening of neurovascular bundle on T2-weighted images (T2WI). Therefore, the assesment of EPE is strongly associated with the experience level of the radiologist [9–11]. However, even with experienced radiologists, the subjective assessment of EPE using T2WI has high specificity but low sensitivity and poor interobserver agreement rates [12,13]. Moreover, only modest improvement was reported regarding the accuracy of EPE diagnosis with the advent of functional imaging sequences such as diffusion-weighted imaging (DWI) and dynamic contrast-enhanced (DCE) images [14]. An objective Mp-MRI parameter for the assesment of EPE is required.

The length of capsular contact (LCC) is defined as the amount of prostate tumor contact with the capsule and is recieved as an independent predictor of EPE [15,16]. It was shown that pathological LCC correlates better with microscopic EPE than the tumor volume [15]. The LCC which was initially presented as an ultrasound (US) based parameter [17], has renewed interest as an objective MRI-based parameter on the diagnosis of EPE. Current studies established that LCC has been a promising Mp-MRI parameter for EPE assesment with good interreader reproducibility and relatively higher accuracy rates [15,16,18–20]. In the majority of these studies, the determination of LCC was based on high resolution T2WI [15,16,19,20]. To the best of our knowledge, there were only 2 studies that included other functional Mp-MRI sequences on LCC determination [18,21]. In one of these studies [18], T2WI and Apparent Diffusion Coefficient (ADC) map were used for determining LCC and the results of this study stated that LCC had higher specificity when using the T2WI than when using the ADC map. The other study evaluated the optimal sequence for measuring LCC and T2WI, ADC map and DCE-MRI were included in the measurements [21]. In this second study, the authors reported that all sequences had relatively equivalent diagnostic performance and they suggested that the highest length of tumor contact with capsule measured from any sequence (maximum LCC) provided better diagnostic performance. There is no agreement on the optimal sequence for measuring LCC between these studies.

The contribution of the other functional Mp-MRI sequences including ADC map and DCE-MRI in the assesment of EPE based on MRI-determined LCC should be further investigated. The aim of this study is to evaluate the optimal Mp-MRI sequence for determining pathological LCC in assesment of EPE of the PCa.

2. Materials and methods

2.1. Patients

This retrospective study received approval from the ethics and research committee of our institution. We searched our institutional databases of pathology, radiology and urology to determine patients with PCa who underwent Mp-MRI of prostate prior to RP between 2012 and 2017. 115 patients were initially enlisted and 10 of them were excluded for the following reasons: missing pathology records (3 patients), long time interval (> 6 months) between Mp-MRI and RP (5 patients), short time interval (< 6 weeks) between prostate biopsy and Mp-MRI (2 patients). Remaining 105 patients with prostate cancer were enrolled in this retrospective study. The demographic data and clinical variables of the included patients were summarized in Table 1.

Table 1
Demographic data and clinical variables of the patients.

Number of Patients	105
Age (years), mean (range)	62 (ranging from 40 to 77)
PSA(ng/mL), mean (range)	7.95 (ranging from 2.10 to 46)
Time interval between MRI and RP (days), mean (range)	31 (ranging from 11 to 137)
Prostate Cancer Risk Groups	105
Low risk group	24
Intermediate risk group	52
High risk group	24
ISUP score	105
ISUP 1	5
ISUP 2	61
ISUP 3	24
ISUP 4	5
ISUP 5	10

PSA = prostate specific antigen, ISUP = International Society of urogenital pathology.

2.2. MRI protocol

All patients were conducted by a 3 T MR scanner (MagnetomSkyra, Siemens Medical Solutions, Erlangen, Germany) and a sixteen-channel phased array surface coil in supine position. During the imaging procedure, 20 mg of butylscopolamine bromide were administered intravenously to avoid artifacts due to bowel peristalsis. In our institute, the Mp-MRI of prostate protocol included triplanar turbo spin-echo T2WI (Repetition/Echo Time (TR/TE) = 3566–3631 ms/100 ms; matrix size = 512 × 352; field of view = 200 mm; slice thickness = 3 mm), free breathing single-shot echo-planar imaging DWI with ADC mapping (TR/TE = 4000/101 ms; matrix size = 192 × 154; field of view = 260 × 260 mm; slice thickness/gap = 3.6 mm/0.3 mm; 22 axial slices; b-values = 0, 50, 100, 200, 400, 600, and 800 s/mm²) with number of excitations = 9) and axial fat-suppressed DCE-MRI (TR/TE = 4.86/1.76 ms; matrix size = 192 × 154; field of view = 260 × 260 mm; slice thickness = 3.6 mm).

2.3. Pathological analysis

All RP specimens underwent fixation with 10% buffered neutral formalin. Then, the specimens were serially sectioned into 3–4 mm intervals by standard step-sectioning and were stained with hematoxylin and eosin. The index lesions were marked on a 16-sector standard prostate diagram by the urogenital pathologist who was blind to any MRI interpretations. The following criteria were used to describe the index lesion: 1-the tumor foci demonstrating EPE were considered as the index lesion; 2- If none of the tumor foci showed EPE, index lesion was considered as the prostate tumor foci with the highest Gleason score or largest tumor volume [15]. After marking the localization of index lesion, the volume, the International Society of Urological Pathology (ISUP) grade groups (Gleason group grade) of index lesion and extra prostatic disease including EPE were also documented. In addition, all RP specimens were reviewed and pathological LCC were calculated with the method that was mentioned by Baco et al. [15].

2.4. Image analysis and determination of LCC

Two radiologist (reader 1, B.B; reader 2, A.O) with 12 and 5 years of experience, respectively in genitourinary radiology independently evaluated the images. The radiologist knew that the patients had RP due to PCa but were blind to any other clinical or pathologic information of patients. At the time of image evaluation, all Mp-MRI sequences including T2W, DCE-MRI and ADC map were available. The radiologists evaluated the images to localize a dominant tumor as defined a mass-like lesion that showed low signal intensity on T2WI and

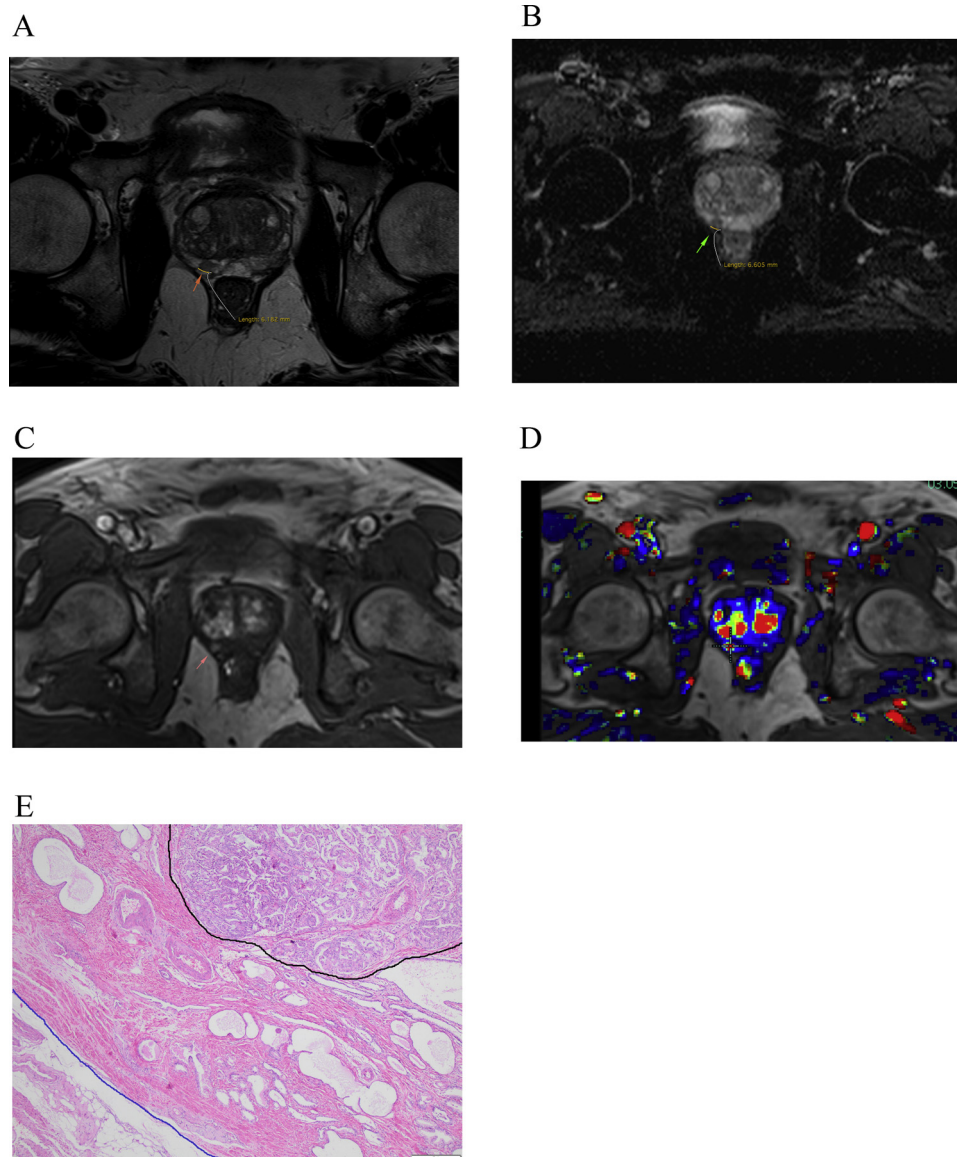


Fig. 1. A 67-year-old man with Gleason score 3 + 4 tumor in right posteromedial peripheral zone (arrow). The length of capsular contact (LCC) on (a) T2W imaging and (b) ADC map by using a digitalized curvilinear ruler tool was represented. There was no contact between tumor and prostate capsule according to DCE-MRI (c, d). In the final pathology (e), the Pca foci (black line) neither had contact with prostate capsule (blue line) nor had extra prostatic extension.

ADC map with or without early contrast enhancement [18]. Then, the radiologist assessed the images including T2WI, DCE-MRI and ADC map to investigate whether or not there was a contact between the dominant tumor and the capsule. In the existence of a contact, the LCC of the dominant lesion was determined which was defined as the maximum length of prostate lesion contact with adjacent prostate capsule among axial images. A curved measurement tool was used as Baco et al. previously delineated to measure the actual contact length between the prostate tumor and adjacent prostate capsule. The LCCs were measured on axial T2WI, ADC map and DCE-MRI, separately. If there was no contact between the tumor and capsule on an individual Mp-MRI sequence or there was no noticeable dominant tumor, the LCC was recorded as 0. The image evaluation and the measurement of the LCC were implemented by using DynaCAD prostate software. Taking the alterations of prostate shape and size due to preservation of the specimen into consideration, the dominant lesions were evaluated and were matched with histopathological diagrams as the reference standard. A lesion was admitted as a matched lesion if it was in the same location on both Mp-MRI and RP specimens.

2.5. Statistical analysis

Statistical analysis was performed using IBM, SPSS software for Windows (v21.0; Chicago, IL). Kolmogorov–Smirnov test was used to examine the normality of LCCs and it was found that all LCCs were not normally distributed ($P < 0.001$). The LCCs of index lesions were compared between radiologists by calculating intra-class correlation coefficient (ICC). Mann–Whitney–U test was used to compare the LCCs in patients with and without EPE. The relationship between the pathological LCC from RP specimens and LCC determined from each Mp-MRI sequences were calculated using Spearman test. Receiver operator characteristic (ROC) curve analysis was performed to compare the ability of all individual Mp-MRI sequences in determining the pathological LCC. The diagnostic accuracy of LCC based on each MRI sequences for EPE diagnosis were also calculated by drawing ROC curves. Delong test was used to compare ROC curves. The most optimal threshold of the LCC for all data sets on EPE diagnosis were determined by using Youden index.

3. Results

3.1. Histopathological results

The mean and median tumor volume of index lesions were 2.14 cm [3] and 1.8 cm [3] (ranging from 0.3 cm [3] to 15.9 cm [3]) based on RP specimens. 24 of 105 patients (22.8%) had evidence of EPE. Capsular contact was found in 86 of 105 patients (81.9%) according to histopathological results. The mean and median value of LCC determined from RP specimens were 13.57 ± 0.999 mm and 14 mm respectively (ranged between 0 mm to 48 mm). The ISUP grade groups of RP specimens were 1 (n = 5), 2 (n = 61), 3 (n = 24), 4 (n = 5) and 5 (n = 10).

3.2. MRI findings

All MRI suspicious dominant lesions corresponded to the index lesions in the RP specimens. For 2 of 105 patients (1.9%), the dominant lesion could not be determined on any Mp-MRI images. For reader-1, in 5 of 105 patients (4.8%); for reader-2, in 6 of 105 patients (5.7%), the dominant tumor was unnoticeable on DCE-MRI. For reader-1, the sensitivity was 100% and specificity was 50% based on T2WI, the sensitivity was 98.8% and specificity was 50% based on ADC map, the sensitivity was 98.8% and specificity was 70.5% based on DCE-MRI. For reader-2, the sensitivity was 100% and specificity was 50% based on T2WI, the sensitivity was 98.8% and specificity was 50% based on ADC map, the sensitivity was 98.8% and specificity was 68.75% based on DCE-MRI. A representative case for demonstrating the relationship between prostate tumor and prostate capsule based on various Mp-MRI sequences was given in Fig. 1 (a–d). The mean and median value of LCC that was measured from all Mp-MRI sequences for both readers were given in Table 2.

Inter-observer agreement was excellent for measuring LCC based on T2WI, ADC map and DCE-MRI between readers. (LCC on T2WI ICC: 0.979, %95, CI: 0.969–0.986; LCC on ADC map ICC: 0.979, %95, CI: 0.969–0.985; LCC on DCE ICC: 0.983, %95, CI: 0.975–0.989). The results of Mann Whitney-U test showed that patients with EPE had longer mean and median LCC than patients without EPE for each Mp-MRI sequences and for both readers. Box and plots that further illustrating the differences between the distribution of LCC with and without EPE with regard to all Mp-MRI sequences for reader-1 and reader-2 were shown in Fig. 2. As shown in figures, the LCC exhibited a broader overlapping between patients with and without EPE on ADC map (reader-1, p = 0.01; reader-2, p = 0.01) when compared with T2WI (reader-1, p = 0.002; reader-2, p = 0.001) and DCE-MRI (reader-1, p = 0.001; reader-2, p = 0.001). Spearman test showed strong correlation between pathological LCC and MRI based LCC for both readers. In addition, LCC based on DCE-MRI showed the strongest correlation with pathological LCC when compared with the other Mp-MRI sequences (Table 3).

ROC curves were drawn to predict the ability of all individual Mp-MRI sequences in determining the pathological LCC (Fig. 3). The areas

under the curve (AUC) of LCC based on DCE-MRI (reader-1: 0.874, %95, CI: 0.763–0.986, p = 0.030; reader-2: 0.862, %95, CI: 0.745–0.978, p = 0.02) were higher than the AUC of LCC based on T2WI (reader-1: 0.836, %95, CI: 0.702–0.969, p = 0.01; reader-2: 0.833, %95, CI: 0.699–0.967, p = 0.01) and ADC map (reader-1: 0.818, %95, CI: 0.696–0.939, p = 0.003; reader-2: 0.835, %95, CI: 0.723–0.946, p = 0.004) for determination of the pathological LCC. The LCC based on T2WI (reader-1: 0.706, %95, CI: 0.609–0.790; reader-2: 0.718, %95, CI: 0.621–0.801), and DCE-MRI (reader-1: 0.715, %95, CI: 0.618–0.800; reader-2: 0.732, %95, CI: 0.635–0.814) showed fair diagnostic accuracy for EPE diagnosis. However, the LCC based on ADC map (reader-1: 0.676, %95, CI: 0.578–0.764; reader-2: 0.663, %95, CI: 0.564–0.752) had poor diagnostic accuracy for EPE diagnosis on the basis of ROC curve analysis. When the ROC curves were compared, only the difference between AUC of LCC based on DCE-MRI and ADC map was statistically significant for reader 2 (reader 2: p = 0.02 for ADC map versus DCE-MRI). However, the AUCs of other LCCs were comparable for both readers in determining the presence of EPE (reader 1: p = 0.27 for ADC map versus DCE-MRI, p = 0.92 for ADC map versus T2WI, p = 0.92 for DCE-MRI versus T2WI; reader 2: p = 0.13 for ADC map versus T2WI, p = 0.86 for DCE-MRI versus T2WI). The optimal threshold value for determining EPE with each Mp-MRI sequence were given in Table 4.

4. Discussion

We evaluated the most optimal Mp-MRI sequence in determining pathological LCC for the diagnosis of EPE. The LCC were more discriminative between the patients with and without EPE when using the T2WI and DCE-MRI than when using the ADC map. The results of the current study showed that the DCE-MRI had highest specificity and almost similar sensitivity when compared to T2WI and ADC map on demonstrating the accurate contact between the prostate tumor and capsule when the RP specimens were taken as the reference standard. We also showed that DCE-MRI were more sensitive and specific than other Mp-MRI sequences in determining the pathological LCC. However, LCC based on DCE-MRI and LCC based on T2WI showed similar performance in diagnosing EPE. Although, DCE-MRI have superiority in accurate determination of pathological LCC, measuring LCC from DCE-MRI had no additional contribution in clinical EPE assessment, according to results of our study.

The results of our study were in accordance with a previous study by Rozenkratz et al. that evaluated LCC based on T2WI and ADC map for EPE diagnosis [18]. The authors of this previous study reported that LCC determination based on T2WI was more sensitive and specific than the LCC determination based on ADC map for assessment of EPE. We also found that ADC map had lower sensitivity and specificity on pathological LCC determination than T2WI. These results may strongly be associated with the greater anatomical distortion and lower spatial resolution of DWI as the authors of the previous study explained. However, Rozenkratz et al. did not determine LCC based on DCE-MRI in their previous report. We found that DCE-MRI had better accuracy in

Table 2

The length of capsular contact according to presence of extra-prostatic extension measured from various Mp-MRI sequences for both readers.

Variables	EPE (+)		EPE (-)		Mean overall LCC (ranging)	Median overall LCC
	Mean LCC (mm \pm stdev)	Median LCC (mm)	Mean LCC (mm \pm stdev)	Median LCC (mm)		
LCC _{T2WI(R-1)}	19.1 \pm 8.2	18.5	13.0 \pm 8.3	13	14.4 \pm 8.7 (ranging 0 to 53)	14
LCC _{T2WI(R-2)}	19.7 \pm 8.6	18	13.3 \pm 8.6	13.5	14.8 \pm 9.2 (ranging 0 to 55)	14
LCC _{ADC(R-1)}	17.9 \pm 9.3	18	12.7 \pm 8.2	13.7	13.9 \pm 8.7 (ranging 0 to 51)	14
LCC _{ADC(R-2)}	19.0 \pm 9.6	19.5	12.9 \pm 8.4	12.5	14.3 \pm 9.1 (ranging 0 to 54)	14
LCC _{DCE(R-1)}	19.1 \pm 9.7	17.7	11.5 \pm 7.1	13.0	13.3 \pm 8.4 (ranging 0 to 40)	14
LCC _{DCE(R-2)}	19.9 \pm 7.6	17.3	11.9 \pm 10.8	12.0	13.7 \pm 9.0 (ranging 0 to 41)	14

LCC = length of capsular contact, EPE = extra-prostatic extension.

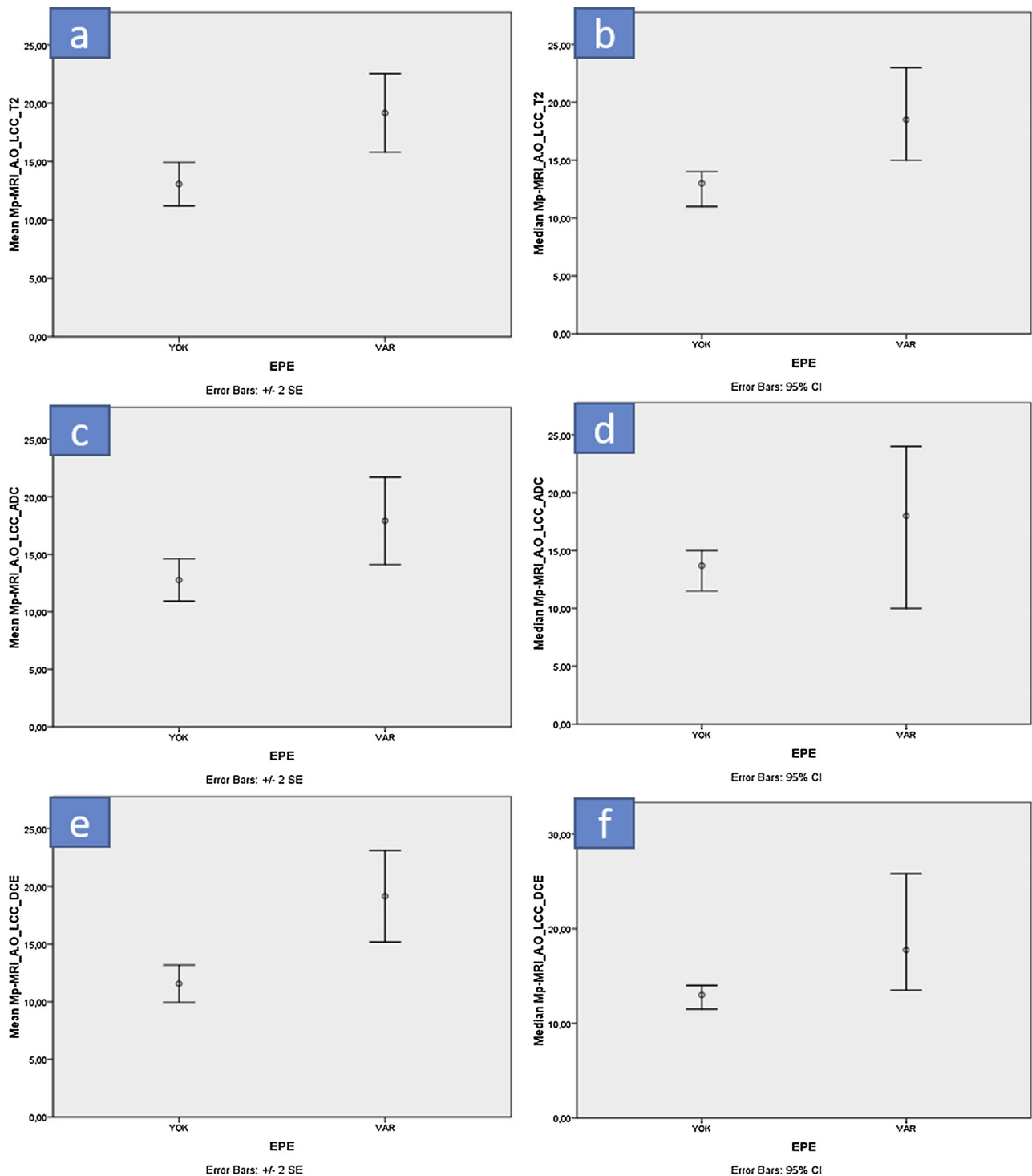


Fig. 2. Box and plots illustrating the differences between the distribution of length of capsular contact with and without ECE with regard to T2WI (a–b), ADC map (c, d) and DCE-MRI (e, f).

pathological LCC determination than the other Mp-MRI sequences. The disadvantages of DWI as anatomical distortion and low spatial resolution were not encountered in DCE-MRI. Furthermore, DCE-MRI has potential of providing information as a functional Mp-MRI sequence in the evaluation of PCa. It was shown that while prostate tumor identification with T2WI were related with Gleason score and tumor size, prostate tumor identification with DCE-MRI was related with the following histological features: inter-mixed benign epithelium, loose stroma and a high malignant epithelium-to-stroma ratio [22]. Some recent studies found that during Pca development, epithelial neoplastic

changes cause alterations on various types of stromal cells. It was also suggested that the alterations in prostate tumor stroma might stimulate angiogenesis and might promote proliferation and invasion. As a result, such alterations of prostate tumor stroma might have an important role in local tumor spread, tumor aggressiveness and patients outcome [23]. The changes in prostate tumor stroma nearby the prostate pseudo-capsule may explain the role of capsular contact in indicating EPE as an independent predictor. In addition, the identification of loose stroma and a high malignant epithelium-to-stroma ratio with DCE-MRI may also explain the superiority of DCE-MRI in determining pathological

Table 3

Spearman correlation matrix is seen between pathological length of capsular contact, T2WI based length of capsular contact, ADC based length of capsular contact and DCE-MRI based length of capsular contact for both readers (correlation is significant at 0.01 level [2-tailed]).

Variables	LCC _{pathological}	LCC _{T2WI(R-1)}	LCC _{T2WI(R-2)}	LCC _{ADC(R-1)}	LCC _{ADC(R-2)}	LCC _{DCE(R-1)}	LCC _{DCE(R-1)}
LCC _{pathological}	1.000	0,708	0,684	0,710	0,701	0,735	0,745
LCC _{T2WI(R-1)}	0,708	1.000	0,965	0,907	0,914	0,852*	0,852
LCC _{T2WI(R-2)}	0,684	0,965	1.000	0,899	0,927	0,853	0,870
LCC _{ADC(R-1)}	0,710	0,907	0,899	1.000	0,965	0,881	0,861
LCC _{ADC(R-2)}	0,701	0,914	0,927	0,965	1.000	0,872	0,868
LCC _{DCE(R-1)}	0,735	0,852	0,853	0,881	0,872	1.000	0,955
LCC _{DCE(R-2)}	0,745	0,852	0,870	0,861	0,868	0,955	1.000

LCC = length of capsular contact, T2WI (R-1)=T2 weighted imaging (reader 1), T2WI (R-2)= T2 weighted imaging reader 2.

ADC (R-1) = Apparent diffusion coefficient (reader 1), ADC (R-2)= Apparent diffusion coefficient (reader 2), DCE (R-1)= Dynamic contrast enhanced (reader 1), DCE (R-2)= Dynamic contrast enhanced (reader 2).

LCC relative to T2WI.

Current studies suggested that DCE-MRI contributed a limited value to T2WI and DWI in tumor detection. Furthermore, DCE-MRI has less impact in cancer detection among the recent guidelines [24–26]. The results of this study showed that DCE-MRI is superior in detecting pathological LCC that might provide a potential clinical usage for this MRI sequence. Nevertheless, measuring LCC from DCE-MRI for clinical EPE assesment had the following shortcomings. Firstly, the diagnostic accuracy for EPE assesment was similar between measuring LCC from T2WI and measuring LCC from DCE-MRI. It seems that the superiority of DCE-MRI in determining pathological LCC have no clinical impact in diagnosing EPE. Secondly, it is well known that performing DCE-MRI have some drawbacks such as its cost and being time consuming. In addition, gadolinium based contrast agents have potential risks such as accumulation in brain and systemic nephrogenic fibrosis. Thirdly, in this current study, the number of invisible tumors in DCE-MRI was more in number than in T2WI and DWI. The high number of invisible prostate tumors in DCE-MRI might be challenging for tumor staging with DCE-MRI. The dominant tumors that were undetected in Mp-MRI were assumed as low-risk prostate cancer and organ-confined disease by some authors [27]. In our study, the undetected tumors were also organ-confined. However, an established study with a large cohort

showed that 29% of invisible tumors with Mp-MRI were ≥ T3 stage [28]. Naturally, when the dominant lesion can not be detected with MRI, it is not possible to evaluate for the purpose of prostate cancer staging.

The current study was in disagreement with the results of a previous study by Woo et al. who compared various Mp-MRI sequences including ADC map, T2WI and DCE in determining LCC for EPE diagnosis. In that previous study, the pathological LCC based on RP specimens and the relationship between the pathological LCC and MRI-determined LCCs were not established. The authors evaluated the diagnostic performance of LCCs from various Mp-MRI sequences in EPE assesment and found that each MRI sequence showed similar accuracy for EPE diagnosis on the basis of ROC curve analysis. They also evaluated the performance when using the maximum LCC measured from any sequence and suggested that the use of maximum LCC yielded better diagnostic performance due to the propensity of MRI in underestimating the pathological tumor volume. However, pathological LCC was assumed as an independent predictor of EPE and had better correlation with EPE than pathological tumor volume. In our study, we observed that DCE-MRI had higher accuracy in determination of pathological LCC than other Mp-MRI sequences. In addition, we showed that DCE-MRI had strongest correlation with pathological LCC when compared with the other Mp-

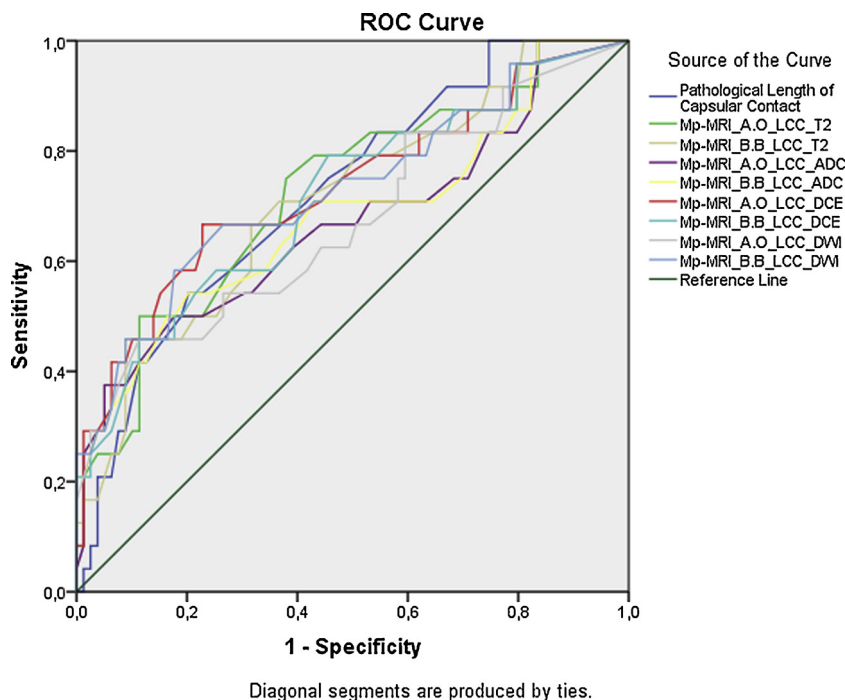


Fig. 3. Receiver operating characteristic analysis showed the ability of T2WI, ADC map and DCE-MRI in determining the pathological length of capsular contact for both readers.

Table 4
The results of receiver operating characteristic curve analysis for LCC in determining extra prostatic extension.

Variables	Cut-Off Value	AUC	Sensitivity	Specificity	P _{value}
LCC-T2w _i (R-1)	14 mm	0.706 (0.609-0.790)	75%	52%	0.0009
LCC-T2w _i (R-2)	13.5 mm	0.718 (0.621-0.801)	75%	52%	0.0004
LCCADC _(R-1)	14 mm	0.676 (0.578-0.764)	66.5%	57%	0.0109
LCC-ADC _(R-2)	13.5 mm	0.663 (0.564-0.752)	71%	55.5%	0.0208
LCC-DCE _(R-1)	13 mm	0.715 (0.618-0.800)	75%	62%	0.0008
LCC-DCE _(R-2)	13 mm	0.732 (0.635-0.814)	79%	54.5%	0.0004

LCC = length of capsular contact, AUC = Area under curve.

MRI sequences. Moreover, the median and mean value of MRI-based LCC and the mean and median value of pathological LCC were very close to each other in our study. According to our results, unlike pathological tumor volume, MRI is able to determine pathological LCC without underestimation or overestimation.

In this study, we showed that all MRI sequences had strong correlation with pathological LCC and the diagnosis of EPE with T2WI and DCE-MRI-based LCC had fair accuracy with good inter-reader reproducibility. Our results were in accordance with the current literature that established fair to good accuracy with reliable to substantial interobserver agreements for EPE diagnosis with MRI-based LCC [15,16,18–21]. The most optimal threshold was found as 13.5 mm with 75% sensitivity and 52% specificity for reader-1 and 13.7 mm with 75% sensitivity and 52% specificity for Reader-2 in predicting EPE in our study cohort. The recent studies that evaluated LCC as an indicator for EPE established quite different median RD values and thresholds, ranging between 6–10 mm to 20 mm. There was no agreement for the most optimal cut-off value in predicting EPE and determination of the optimal threshold becomes an important debate recently. The threshold value of the current study was closest to the threshold value of 12.5 mm established by Kongnyuy et al [16] This might be due to the fact that both studies had close similarities in patient selection and study cohort. In both studies, the patients with prostate cancer who underwent RP and had Mp-MRI scan prior to surgery were included.

Though, our study had limitations. First, the study was performed in a retrospective design that may introduce biases in population selection. Second, our study population consisted of the patients who either had biopsy prior to Mp-MRI or the biopsy-naive patients who were initially evaluated with mp-MRI. Post-biopsy hemorrhage may prevent accurate evaluation of Mp-MRI for Pca staging by leading to overestimation of EPE due to its similar appearance with Pca [29]. According to the recent guidelines, a delay of 6 weeks or longer is recommended for MRI examination after biopsy for prostate cancer staging [24]. Consequently, we included the patients who had a time interval of at least 6 weeks between prostate biopsy and MRI examination in our study. However, some recent studies found that the extent of post-biopsy hemorrhage on prostate gland was not sufficiently absorbed over time. In addition, it was also reported that hemorrhage after biopsy did not prevent the evaluation of prostate cancer staging with Mp-MRI [30,31]. On the contrary, in another study, it was reported that the ability of EPE diagnosis with MRI-based LCC was lower in patients when the Mp-MRI was evaluated after biopsy when compared with the patients who were initially evaluated with Mp-MRI [18]. The diagnostic accuracy of MRI-based LCC was not evaluated separately in patients with and without biopsy prior to MRI examination, since the number of patients with EPE was insufficient for performing subgroup analysis. Third, our study cohort consisted of the patients who underwent Mp-MRI prior to RP due to the fact that we used RP specimens as the reference standard. Therefore, the patients who were treated with other methods such as active surveillance and radiotherapy or hormonal therapy were not included in this study. The number of patients with low volume Gleason score 3 + 3 cancer and the patients with high tumor burden and high risk cancer were limited in our study. Prospective multi-center studies with a larger study population is still

needed.

In conclusion, the length of tumor contact with the capsule based on T2WI and DCE-MRI showed fair accuracy with good inter-reader reproducibility in EPE diagnosis which means that LCC seems to be a useful and objective MRI-based parameter for assessing EPE on Pca. Moreover, DCE-MRI had highest specificity on demonstrating the accurate contact between the prostate tumor and capsule and showed the highest accuracy in predicting pathological LCC. However, it should be noted that there was no difference between measuring LCC from T2WI and DCE-MRI in terms of clinical EPE assessment.

Funding

This research did not receive any specific grant from funding agencies in the public, commercial, or not-for-profit sectors.

Conflicts of interest

The authors have no potential conflicts of interest related with this article.

Acknowledgement

We thank Cavit Kerem Kayhan, pathology technician for assistance with reviewing all the pathology databases of our institution that gave great contribution to this manuscript.

References

- [1] M.K. Tollefson, R.J. Karnes, L.J. Rangel, E.J. Bergstralh, S.A. Boorjian, The impact of clinical stage on prostate cancer survival following radical prostatectomy, *J. Urol.* 189 (2013) 1707–1712, <https://doi.org/10.1016/j.juro.2012.11.065>.
- [2] M.A. Rosen, L. Goldstone, S. Lapin, T. Wheeler, P.T. Scardino, Frequency and location of extracapsular extension and positive surgical margins in radical prostatectomy specimens, *J. Urol.* 148 (1992) 331–337, [https://doi.org/10.1016/S0022-5347\(17\)36587-4](https://doi.org/10.1016/S0022-5347(17)36587-4).
- [3] G. Godoy, B.U. Tareen, H. Lepor, Site of positive surgical margins influences biochemical recurrence after radical prostatectomy, *BJU Int.* 104 (2009) 1610–1614, <https://doi.org/10.1111/j.1464-410X.2009.08688.x>.
- [4] A. Heidenreich, J. Bellmunt, M. Bolla, et al., EAU guidelines on prostate cancer. Part 1: screening, diagnosis, and treatment of clinically localised disease, *Eur. Urol.* 59 (2011) 61–71, <https://doi.org/10.1016/j.eururo.2010.10.039>.
- [5] S.F. Shariat, P.I. Karakiewicz, C.G. Roehrborn, M.W. Kattan, An updated catalog of prostate cancer predictive tools, *Cancer.* 113 (2008) 3075–3099, <https://doi.org/10.1002/cncr.23908>.
- [6] J. Salerno, A. Finelli, C. Morash, et al., Multi-parametric magnetic resonance imaging for pre-treatment local staging of prostate cancer: a Cancer care Ontario clinical practice guideline, *Can. Urol. Assoc. J.* 10 (2016) 332–339, <https://doi.org/10.5489/cuaj.3823>.
- [7] J.O. Barentsz, J. Richenberg, R. Clements, et al., ESUR prostate MR guidelines 2012, *Eur. Radiol.* 22 (2012) 746–757, <https://doi.org/10.1007/s00330-011-2377-y>.
- [8] S.C. Eberhardt, S. Carter, D.D. Casalino, et al., ACR Appropriateness Criteria prostate cancer—pretreatment detection, staging, and surveillance, *J. Am. Coll. Radiol.* 10 (2013) 83–92, <https://doi.org/10.1016/j.jacr.2017.02.026>.
- [9] M.R. Engelbrecht, G.J. Jager, R.J. Laheij, A.L. Verbeek, H.J. van Lier, J.O. Barentsz, Local staging of prostate cancer using magnetic resonance imaging: a meta-analysis, *Eur. Radiol.* 12 (2002) 2294–2302, <https://doi.org/10.1007/s00330-002-1389-z>.
- [10] M. Mullerad, H. Hricak, L. Wang, H.N. Chen, M.W. Kattan, P.T. Scardino, Prostate Cancer: detection of extracapsular extension by genitourinary and general body radiologists at MR imaging, *Radiology* 232 (2004) 140–146, <https://doi.org/10.1148/radiol.2321031254>.

- [11] Jurgen J. Fütterer, R. Marc, et al., Staging prostate Cancer with dynamic contrast-enhanced endorectal MR imaging prior to radical prostatectomy: experienced versus less experienced readers, *Radiology* (2005) 541–549, <https://doi.org/10.1148/radiol.2372041724>.
- [12] K.H. Hole, K. Axcrone, A.K. Lie, et al., Routine pelvic MRI using phased array coil for detection of extraprostatic tumour extension: accuracy and clinical significance, *Eur. Radiol.* 23 (2013) 1158–1166, <https://doi.org/10.1007/s00330-012-2669-x>.
- [13] J.V. Hegde, M.H. Chen, R.V. Mulkern, F.M. Fennessy, A.V. D'Amico, C.M. Tempany, Preoperative 3-Tesla multiparametric endorectal magnetic resonance imaging findings and the odds of upgrading and upstaging at radical prostatectomy in men with clinically localized prostate cancer, *Int J. Radiat. Oncol. Biol. Phys.* (2013) e101–e107, <https://doi.org/10.1016/j.ijrobp.2012.08.032>.
- [14] M. de Rooij, E.H. Hamoen, J.A. Witjes, J.O. Barentsz, M.M. Rovers, Accuracy of magnetic resonance imaging for local staging of prostate cancer: a diagnostic meta-analysis, *Eur. Urol.* 70 (2016) 233–245, <https://doi.org/10.1016/j.eururo.2015.07.029>.
- [15] E. Baco, E. Rud, L. Vlatkovic, et al., Predictive value of magnetic resonance imaging determined tumor contact length for extracapsular extension of prostate cancer, *J. Urol.* 193 (2015) 466–472, <https://doi.org/10.1016/j.juro.2014.08.084>.
- [16] M. Kongnyuy, A. Sidana, A.K. George, et al., Tumor contact with prostate capsule on magnetic resonance imaging: a potential biomarker for staging and prognosis, *Urol. Oncol.* 35 (30) (2016), <https://doi.org/10.1016/j.urolonc.2016.07.013> e1–8.
- [17] O. Ukimura, P. Troncoco, E.I. Ramirez, et al., Prostate cancer staging: correlation between ultrasound determined tumor contact length and pathologically confirmed extraprostatic extension, *J. Urol.* 159 (1998) 1251–1259, [https://doi.org/10.1016/S0022-5347\(01\)63575-4](https://doi.org/10.1016/S0022-5347(01)63575-4).
- [18] A.B. Rosenkrantz, A.K. Shanbhogue, A. Wang, et al., Length of capsular contact for diagnosing extraprostatic extension on prostate MRI: assessment at an optimal threshold, *J. Magn. Reson. Imaging* 43 (2015) 990–997, <https://doi.org/10.1002/jmri.25040>.
- [19] S. Krishna, C.S. Lim, M.D.F. McInnes, et al., Evaluation of MRI for diagnosis of extraprostatic extension in prostate Cancer, *J. Magn. Reson. Imaging* 47 (2018) 176–185, <https://doi.org/10.1002/jmri.25729>.
- [20] G. Mendez, B.R. Foster, X. Li, et al., Endorectal MR imaging of prostate cancer: evaluation of tumor capsular contact length as a sign of extracapsular extension, *Clin. Imaging* 50 (2018) 280–285, <https://doi.org/10.1016/j.clinimag.2018.04.020>.
- [21] S. Woo, S.Y. Kim, J.Y. Cho, S.H. Ki, Length of capsular contact on prostate MRI as a predictor of extracapsular extension: which is the most optimal sequence? *Acta Radiol.* 58 (2017) 489–497, <https://doi.org/10.1177/0284185116658684>.
- [22] A.B. Rosenkrantz, S. Mendrinis, J.S. Babb, S.S. Taneja, Prostate cancer foci detected on multiparametric magnetic resonance imaging are histologically distinct from those not detected, *J. Urol.* 187 (2012) 2032–2038, <https://doi.org/10.1016/j.juro.2012.01.074>.
- [23] C. Hägglöf, A. Bergh, The stroma: a key regulator in prostate function and malignancy, *Cancers (Basel)* 4 (2012) 531–548, <https://doi.org/10.3390/cancers4020531>.
- [24] J.C. Weinreb, J.O. Barentsz, P.L. Choyke, F. Cornud, M.A. Haider, K.J. Macura, et al., PI-RADS prostate imaging - reporting and data system: 2015, version 2, *Eur. Urol.* 69 (2016) 16–40, <https://doi.org/10.1016/j.eururo.2015.08.052>.
- [25] J.O. Barentsz, J.C. Weinreb, S. Verma, H.C. Thoeny, C.M. Tempany, F. Shtern, et al., Synopsis of the PI-RADS v2 guidelines for multiparametric prostate magnetic resonance imaging and recommendations for use, *Eur. Urol.* 69 (2016) 41–49, <https://doi.org/10.1016/j.eururo.2015.08.038>.
- [26] Prostate Cancer: Diagnosis and Treatment. Clinical Guideline, National Institute for Health and Care Excellence, 2015, <https://www.nice.org.uk/guidance/cg175/evidence>.
- [27] D.M. Somford, E.H. Hamoen, J.J. Fütterer, et al., The predictive value of endorectal 3 Tesla multiparametric magnetic resonance imaging for extraprostatic extension in patients with low, intermediate and high risk prostate cancer, *J. Urol.* 190 (2013) 1728–1734, <https://doi.org/10.1016/j.juro.2013.05.021>.
- [28] S.H. Lee, K.C. Koo, D.H. Lee, B.H. Chung, Nonvisible tumors on multiparametric magnetic resonance imaging does not predict low-risk prostate cancer, *Prostate Int.* 3 (2015) 127–131, <https://doi.org/10.1016/j.pnil.2015.09.005>.
- [29] S. White, H. Hricak, R. Forstner, et al., Prostate cancer: effect of post-biopsy hemorrhage on interpretation of MR images, *Radiology* 195 (1995) 385–390, <https://doi.org/10.1148/radiology.195.2.7724756>.
- [30] A.R. Sharif-Afshar, T. Feng, S. Koopman, C. Nguyen, Q. Li, E. Shkolyar, R. Saouaf, H.L. Kim, Impact of post prostate biopsy hemorrhage on multiparametric magnetic resonance imaging, *Can. J. Urol.* 22 (2015) 7698–7702.
- [31] M.H. Choi, S.E. Jung, Y.H. Park, J.Y. Lee, Y.J. Choi, Multi-parametric MRI of prostate cancer after biopsy: little impact of hemorrhage on tumor staging, *Investig. Magn. Reson. Imag.* 21 (2017) 139–147, <https://doi.org/10.13104/imri.2017.21.3.139>.